Materials Chemistry and Physics 316 (2024) 129106

Contents lists available at ScienceDirect

Materials Chemistry and Physics

journal homepage: www.elsevier.com/locate/matchemphys

The effect of property contrast in two-component piezoelectric composites

Nihal Thafeem Ahmed Faheem Ahmed *, John E. Huber

Department of Engineering Science, University of Oxford, 17 Parks Road, Oxford, OX1 3PJ, UK

HIGHLIGHTS

- Property contrast for two-component piezocomposites explored.
- Uniform contrast offers realizable functional performance enhancements.
- Minimizing material moduli of inclusions boosts transducer figure of merit.
- Biased contrast offers inaccessible performance boosts.
- Property contrast captures functional performance of a real world ceramic.

ABSTRACT

A Mori - Tanaka model of piezoelectric composites is used to study the effect of property contrast between the components of a two-component composite. The composite comprises a piezoelectric matrix and piezoelectric inclusions whose property values are scaled from those of the matrix. The scaling method allows a wide range of material combinations to be approximated without using explicit properties of specific materials. Additionally, the aspect ratio and volume fraction of inclusions is varied to seek optimum values of the piezoelectric coefficients in the composite. It was found that scaling the properties in the electroelastic moduli reveals significant results for the piezoelectric performance coefficients $d_h g_h$, κ_{33}, g_{33} and k_t. By varying the material scaling factors alongside the inclusion aspect ratio it is demonstrated that giant enhancements of the transducer figure of merit $d_h g_h$ could potentially be achieved through composite design. This approach identifies some novel opportunities for optimised piezoelectric composites.

1. Introduction

Piezoelectric composites comprising two components (one of which is allocated the role of the matrix and the other, the inclusion), at least one of which is piezoelectric, have found extensive use in applications such as ultrasonic medical imaging devices and sonar transducers [1]. A longstanding challenge in the field is to optimise or maximise piezoelectric effects, given the limitations of the known monolithic piezoelectrics. It is well known that composites can have greater values of certain piezoelectric coefficients than either of the constituent components [2]. A rich literature exists on various aspects of piezoelectric composites, which offers insight into how to obtain the best performance for specific applications. These studies have involved a range of parameters including the properties of the components [3], interface effects [4], polarization orientation [5], porosity [6], the number and type of distinct components [7], the orientation of inclusions [8] and inclusion distribution [9], to name a few. By varying these parameters, it is possible to explore a vast material design space and the present work aims to demonstrate that surprising design insights can still emerge from systematic exploration of this space. To this end, a Mori - Tanaka self-consistent scheme is employed to perform micromechanical analyses on two-component composites. In the present work, the approach focuses on the effects of the property contrast between the constituent components as a generic way of capturing a variety of material behaviour and indicating the influence of composite design on the piezoelectric properties of interest. This analytical approach is advantageous in providing a rapid assessment of the effect of parameter variation, thereby enabling a wide range of composite designs to be explored. Accuracy checks were carried out in selected cases using other homogenization schemes, and comparison with results in the literature.

One of the first studies of a piezoelectric composite using micromechanical analysis was undertaken by Dunn and Taya [2], using the Eshelby inclusion model and Mori - Tanaka mean-field theory [10]. This proved to be advantageous over earlier attempts at modelling such composites [11] in that a great variety of composite features could be taken into consideration when computing the effective behaviour. The consequences of varying the aspect ratio of inclusions, their spatial orientations, volume fractions and porosity were all explored. Among

* Corresponding author.
E-mail addresses: nihal.faheemahmed@lincoln.ox.ac.uk (N.T.A. Faheem Ahmed), john.huber@eng.ox.ac.uk (J.E. Huber).

https://doi.org/10.1016/j.matchemphys.2024.129106
Received 24 April 2023; Received in revised form 27 November 2023; Accepted 19 February 2024
Available online 20 February 2024

many findings, it was demonstrated that porous ceramics offer better piezoelectric performance in some cases than their monolithic counterparts. This result is remarkable in that a reduction in the volume fraction of the active piezoelectric component is beneficial to certain piezoelectric properties. Della and Shu [12] exploited the versatility of the method by modelling a hierarchical composite with porous piezoelectric and polymer matrices. Significant improvements in the piezoelectric transducer figure of merit were reported. Porosity has received increased attention in the literature with Zhang et al. [13] reporting the hydrostatic transducer performance of porous piezoelectric ceramics to be superior to that of bulk materials. An expansion on the modelling work has followed with the introduction of additional attributes such as interface effects and poling orientation [14]. The Mori - Tanaka theory has also been demonstrated to have reasonable agreement with finite element calculations [15]. The versatility, reliability and ease of computation makes this approach favourable for piezoelectric composites. One limitation, however, is that local inclusion interactions at high volume fractions are not adequately captured; this limits the validity to inclusion volume fractions up to about 0.5 [16].

The modelling results in the literature typically focus on specific material combinations such as PZT-epoxy composites. However, given that many material combinations are possible, the broader picture of how material property contrast contributes to performance in piezoelectric composites has not been fully explored. Some studies have used property contrast as a parameter [17] for optimising simulation size, but an investigation of property contrast on the performance of piezoelectric composites was not found in the literature. A similar concept of using ratios of electromechanical moduli of the components in a 1–3 piezocomposite was proposed nearly two decades ago by Topolov et al., albeit to characterize non-monotonic volume fraction dependencies of the overall composite properties [18]. While it is well-known that extreme property contrast can be useful, as manifested in porous ceramics, it remains an open question whether moderate contrast, or contrast in particular properties (dielectric, piezoelectric or elastic moduli) has advantages.

To isolate the influence of the property contrast between the components in this work, we use the concept of scaled material properties, with two distinct types of scaling applied: uniform scaling of the entire electroelastic modulus (referred to here as α scaling), or a biased scaling applied to all the elements of just one of the elastic, piezoelectric or dielectric tensors (referred to here as β scaling). A composite comprising a piezoelectric matrix containing inclusions of the same material subjected to α or β scaling is studied using Mori - Tanaka mean field theory. The scaling factors are varied over a wide range from 10^{-2} to 10^{2} representing fictitious materials which may have either very high or very low coefficient values in any one or all of the elastic, dielectric and piezoelectric tensors. At first sight such extremes of contrast may seem unrepresentative of real materials. However, piezoelectric composites comprising piezoceramic inclusions in a polymer matrix may have contrast of order 10^{2} or more in certain properties. Furthermore, α scaling of 10^{-2} gives results similar to the effects of porosity. The results obtained can thus be generalized to a wide variety of piezoceramics and their composites, enabling comparison with prior studies. Methods for achieving significant improvements in other properties are also identified.

2. Models

The models employed in this work are based on the equilibrium laws of electrostatics and solid mechanics. Maxwell's laws applied to electrostatics in the absence of free charge can be stated in differential form as

$$D_{i,i} = 0 \tag{1}$$

$$\varepsilon_{ijk} E_{j,k} = 0 \tag{2}$$

where the electric field, and electric displacement are denoted by E_i and D_i, respectively. Equations (1) and (2) [19] imply the continuity of the normal component of the electric displacement through interfaces and continuity of the tangential component of the electric field across interfaces. Note that the Levi-Civita connection ε_{ijk} is in use in (2). Similarly, equilibrium of stresses σ_{ij}, in the absence of body forces, and compatibility of strains, ε_{ij}, can be expressed as

$$\sigma_{ij,j} = 0 \tag{3}$$

$$\varepsilon_{ijk}\varepsilon_{pqr} u_{j,qkr} = 0 \tag{4}$$

Equations (3) and (4) [19,20] imply continuity of tractions through interfaces and continuity of the displacement field, u_j. Now consider a two-component composite in which each component comprises a piezoelectric material with linear constitutive response of the form:

$$\sigma_{ij} = C_{ijmn}\varepsilon_{mn} + e_{nij}(-E_n) \tag{5}$$

$$D_i = e_{imn}\varepsilon_{imn} - \kappa_{in}(-E_n) \tag{6}$$

where the stiffness tensor C_{ijmn} is measured at constant electric field and the dielectric permittivity tensor κ_{in} is measured at constant strain. Following Barnett and Lothe [21], a compact notation is adopted in the form

$$\Sigma_{iJ} = E_{iJMn} Z_{Mn} \tag{7}$$

where the capital indices run from 1…4, with all other indices running from 1…3. Also,

$$Z_{Mn} = \begin{cases} \varepsilon_{mn}, & M = 1,2,3 \\ E_n, & M = 4 \end{cases} \tag{8}$$

and

$$\Sigma_{iJ} = \begin{cases} \sigma_{ij}, & J = 1,2,3 \\ D_i, & J = 4 \end{cases} \tag{9}$$

The electroelastic modulus of a piezoelectric solid can be given a similar representation

$$E_{iJMn} = \begin{cases} C_{ijmn}, & J,M = 1,2,3 \\ e_{nij}, & J = 1,2,3, M = 4 \\ e_{imn}, & J = 4, M = 1,2,3 \\ -\kappa_{in}, & J,M = 4 \end{cases} \tag{10}$$

For later use the collection of identity tensors I_{MnAb} is defined in terms of the Kronecker delta δ_{bn} by

$$I_{MnAb} = \begin{cases} \frac{1}{2}(\delta_{am}\delta_{bn} + \delta_{an}\delta_{bm}), & A,M = 1,2,3 \\ 0, & A = 1,2,3, M = 4 \\ 0, & A = 4, M = 1,2,3 \\ \delta_{bn}, & A,M = 4 \end{cases} \tag{11}$$

The composites are modelled as a collection of ellipsoidal inclusions embedded in an infinite matrix, according to the wellestablished theories of Mori - Tanaka and Hill [2,22]. In each case, the Eshelby tensor [23] is used to represent the interaction between inclusions and the surrounding matrix material. The extension of Eshelby's theory to incorporate electric fields and electric displacements [24] enables its use in the micromechanical analysis of piezoelectric composites. The electroelastic equivalent of the Eshelby tensor is a collection of 4 tensors that relate the strain and electric field ε_{mn}, E_n in the transformed inclusion to the prescribed eigenstrain and electric displacement-free electric field $\varepsilon^*_{mn}, E^*_n$:

$$\begin{pmatrix} \varepsilon_{mn} \\ -E_n \end{pmatrix} = \begin{pmatrix} S^{\varepsilon\varepsilon}_{mnab} & S^{\varepsilon E}_{bmn} \\ S^{E\varepsilon}_{nab} & S^{EE}_{bn} \end{pmatrix} \begin{pmatrix} \varepsilon^*_{ab} \\ -E^*_b \end{pmatrix} \tag{12}$$

Or, in compact notation

$$Z_{Mn} = S_{MnAb} Z^*_{Ab} \tag{13}$$

where Z_{Mn} is defined as in equation (8). The three principal radii of the ellipsoidal inclusion may take on any values. However, as the theories employed are scale independent, only the ratios are of significance. Explicit expressions have been derived in particular limiting cases [25]. To enable a more general range of cases, the Eshelby tensors are numerically computed in the current work using Gaussian Quadrature. A detailed derivation of the Eshelby tensors in equation (12) can be found in the work of Dunn et al. [2].

2.1. Mori - Tanaka mean field theory

The Mori - Tanaka mean field theory views the piezoelectric composite as a combination of two distinct components with a clearly defined role of matrix and inclusion allocated to them. The resulting homogenization gives overall effective electromechanical properties E^o as [2]

$$E^o_{bAMn} = E^M_{bAPq}\left(I_{PqMn} + fD^{-1}_{PqiJ}\left(E^P_{iJMn} - E^M_{iJMn}\right)\right) \tag{14}$$

where the electroelastic moduli of the matrix and inclusion are given by E^M_{iJMn} and E^P_{iJMn}, respectively, while D_{iJAb} is given by

$$D_{iJAb} = (1-f)\left(E^P_{iJMn} - E^M_{iJMn}\right)S_{MnAb} + E^M_{ijAb} \tag{15}$$

Here f is the volume fraction of the inclusions. Because the Mori - Tanaka theory identifies one component as a connected matrix and the other component as isolated inclusions, exchanging the matrix and inclusion components results in a composite with different properties.

2.2. Hill's self-consistent scheme

For comparison with the Mori - Tanaka scheme, selected calculations were made using the self-consistent formulation due to Hill [22] which differs from the Mori - Tanaka scheme in that each material component of the composite enters the analysis on the same footing. Hill's scheme has previously been used for the representation of piezoelectric and ferroelectric polycrystals [26]. A constitutive equation of the form of (7) holds for each component. To compute the overall effective properties E^o_{iJKl}, Hill's scheme provides the averaging relationship,

$$E^o_{iJKl} = \overline{E_{iJRs}A_{RsKl}} \tag{16}$$

where the over-bar implies a volume average over the component, and A_{RsKl} is a collection of concentration tensors relating the average strain and electric field in a single inhomogeneity to the average strain and electric field in the composite such that

$$Z_{Ij} = A_{IjKl}\overline{Z}_{Kl} \tag{17}$$

The concentration tensors A_{RsKl} are computed using the Eshelby formalism following a procedure outlined by Hill [22,26]. The scheme is self-consistent, in that each component of the composite is treated as if it comprises ellipsoidal inhomogeneities in a matrix whose properties are those of the composite itself. Consequently, the method does not provide explicit expressions for the overall moduli of the composite and iteration is employed.

2.3. Laminate limit and property scaling

In the limit $\frac{c}{a} \to 0$, with $a = b$, the Eshelby inclusions become equivalent to flat layers and the composite is equivalent to a laminate. In this case, a comparison with Mori - Tanaka theory is provided by adopting a variant of the approach presented by Liu et al. [27] to model piezoelectric laminates. Continuity of the stress and electric displacement components normal to each interface between layers is assumed, as is the continuity of strain and electric field components tangential to each interface. The constitutive equation (7) can then be re-cast as

$$\begin{pmatrix} \Sigma_\perp \\ \Sigma_\parallel \end{pmatrix} = \begin{pmatrix} P & Q \\ Q^T & R \end{pmatrix} \begin{pmatrix} Z_\perp \\ Z_\parallel \end{pmatrix} \tag{18}$$

When the interface between layers of the laminate is normal to the x_3 axis, $\Sigma_\perp = [\sigma_{33}, \sigma_{23}, \sigma_{13}, D_3]$, $\Sigma_\parallel = [\sigma_{11}, \sigma_{22}, \sigma_{12}, D_1, D_2]$, $Z_\perp = [\varepsilon_{33}, \varepsilon_{23}, \varepsilon_{13}, -E_3]$ and $Z_\parallel = [\varepsilon_{11}, \varepsilon_{22}, \varepsilon_{12}, -E_1, -E_2]$. The components of the electroelastic modulus E_{iJKl} are accordingly re-arranged in the P, Q and R matrices. Noting that $\Sigma_\perp$ and $Z_\parallel$ are equal in all layers enables a rearrangement of (7) followed by volume averaging, which gives explicit expressions for the effective material moduli P^o, Q^o and R^o of the composite [27]:

$$P^o = \left(\overline{P^{-1}}\right)^{-1} \tag{19}$$

$$Q^o = P^o\overline{P^{-1}Q} \tag{20}$$

$$R^o = \overline{Q^T P^{-1}}Q^o + \overline{R - Q^T P^{-1}Q} \tag{21}$$

Equations 19–21 can be further simplified in the case of a two-component laminate in which one component has properties that are linearly scaled from the other such that $P^2 = \alpha P^1, Q^2 = \alpha Q^1$ and $R^2 = \alpha R^1$. Then, setting P^1, Q^1, R^1 to P, Q and R, respectively, gives

$$P^o = \gamma P \tag{22}$$

$$Q^o = \gamma Q \tag{23}$$

$$R^o = Q^T P^{-1} Q\left(\gamma - \gamma^{-1}\right) + \frac{1}{\gamma}R \tag{24}$$

where

$$\gamma = \frac{1}{1 - f + \frac{f}{\alpha}} \tag{25}$$

$$\gamma^{-1} = 1 - f + \alpha f \tag{26}$$

with f and α denoting volume fraction of inclusion component and the scaling factor, respectively. Two distinct types of scaling of the electromechanical moduli will be considered to generate the moduli of the inclusion material: α-type scaling is a uniform scaling of the moduli such that

$$E^P = \alpha E^M \tag{27}$$

We also consider a biased scaling, referred to here as β-type scaling, applied individually to elastic, piezoelectric or dielectric moduli, such that

$$\beta(C) \Longrightarrow E^P_{iJMn} = \begin{pmatrix} \beta C^M_{ijmn} & e^M_{imn} \\ e^M_{nij} & \kappa^M_{in} \end{pmatrix} \tag{28}$$

$$\beta(e) \Longrightarrow E^P_{iJMn} = \begin{pmatrix} C^M_{iJMn} & \beta e^M_{imn} \\ \beta e^M_{nij} & \kappa^M_{in} \end{pmatrix} \tag{29}$$

$$\beta(\kappa) \Longrightarrow E^P_{iJMn} = \begin{pmatrix} C^M_{ijmn} & e^M_{imn} \\ e^M nij & \beta\kappa^M_{in} \end{pmatrix} \tag{30}$$

In each case, for practical calculations, we limited the range of scaling to $10^{-2} \leq \beta, \alpha \leq 10^2$. Note that (28–30) are not fully independent in that a combination of scaling operations using (28–29) can produce

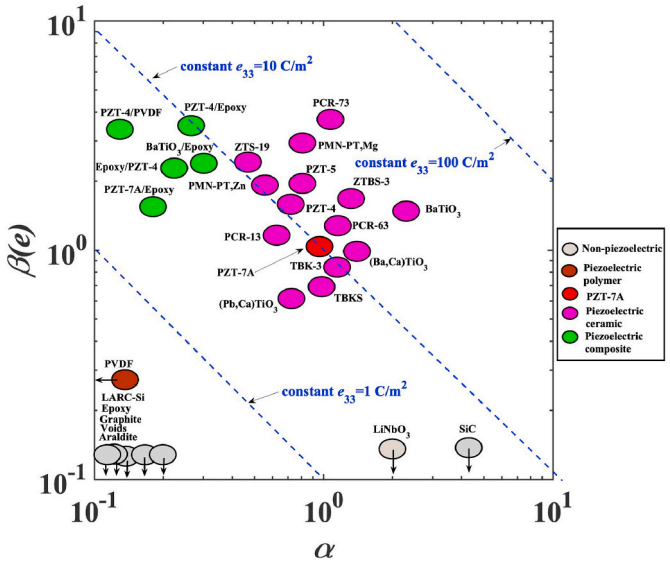

Fig. 1. Illustration of property scaling on reference materials. Approximate α and β (e) values representing a variety of piezoelectrics and other materials are shown.

the equivalent of (30). Furthermore, the existence of non-dimensional groups of the form $\frac{e^2}{C\kappa}$ implies relations between the scaling effects from (28–30). For simplicity we present results for each individual scaling, whilst recognizing similarities. There are also thermodynamic limits to the β scaling achievable in real materials due to the requirement for positive definiteness of the material moduli. These limitations are indicated in the results by using dashed lines when any eigenvalue of the matrix of material moduli becomes negative. An illustration of the use of α and $\beta(e)$ scaling on a base material equivalent to PZT-7A can be seen in Fig. 1. Note that there are also fibrous piezoelectric composites (50 percent inclusion/50 percent matrix combinations) included to serve for comparison. The scaling can be used to approximate a variety of materials: elastic dielectrics without piezoelectricity correspond to $\beta(e) = 0$. Voids have $\beta(C) = 0, \beta(e) = 0, \beta(\kappa) \ll 1$ and correspond to a combination of $\alpha \ll 1$ and $\beta = 0$. Several common piezoelectric materials [28] cluster close to $\alpha = \beta = 1$. Note that arrows near certain materials imply that the materials are further along the axis in the appropriate direction. For convenience of plotting in Fig. 1, we approximate $\alpha = C_{33}/\, C_{33,PZT-7A}$ and $\beta(e) = e_{33}/\alpha e_{33,PZT-7A}$. A more accurate representation of a range of materials would require a variation of all three β coefficients.

2.4. Problem definition

The composite to be analysed consists of general combinations of piezoelectric inclusions in a piezoelectric matrix. We choose material moduli similar to those of a typical piezoelectric, PZT-7A [11], as the base material. This is representative of a ceramic with hexagonal 6 mm symmetry [2]. Each component of the composite is chosen to be poled along the global x_3 direction as shown in Fig. 2. For initial exploration of the effect of the aspect ratio of inclusions, only the c/a ratio is varied, keeping $a = b$, and the major axis of each ellipsoidal inclusion is taken to be aligned with the x_3 direction.

Results for varying aspect ratios of the inclusions will be presented. Effective properties for various piezoelectric coefficients were computed using the Mori - Tanaka model (14) and for limiting cases where $c/a \to 0$, laminate theory (22–24) was used for a consistency check. Hill's homogenization scheme was used to check specific cases. Note that all results are normalize relative to a monolithic piezoelectric material, equivalent to the unscaled base material such that for each coefficient X,

$$X^* = X_{calculated}/X_{base\ ceramic}.$$

The entire code was written and executed in MATLAB®.

3. Results and discussion

3.1. Validation of Mori - Tanaka homogenization method

In order to encourage confidence in the results obtained from the Mori - Tanaka calculations, some standard results first produced by Dunn et al. [2] will be re-computed using the Mori - Tanaka model as implemented in the present work, along with some finite element results for simple composite designs. Note that, for the case of the d_{33} coefficient in Fig. 3(b), experimental results from Chan et al. [29] have been used to compare with theoretical calculations from the Mori - Tanaka model. The results in Fig. 3a-d match closely with those produced by Dunn et al. [2]. For the COMSOL calculations, a cube of dimensions 1.0x1.0 × 1.0 mm^3 was used to model the polymer matrix material. The PZT-4 inclusions were chosen to be spherical. In order to compute the d_{33} and d_{31} coefficients presented in Fig. 3, the expression $d_{3i} = \Delta t_i/E$ was used, where Δt is the change in dimensions of the cube along the i axis and E is the applied electric field in the appropriate direction. See Table 1 for material properties used in calculations.

Though good agreement can be found between the COMSOL and Mori - Tanaka calculations, there is a high discrepancy at inclusion volume fraction $v_f \sim 0.5$ (Fig. 3e-f). This may be attributed to the inability of the Mori - Tanaka model to rigorously account for the touching of inclusions at such high volume fractions [16]. Additionally, as noted by Dunn et al. [16], the Mori - Tanaka model is strictly valid only for dilute or moderate volume fractions ($v_f < 0.5$).

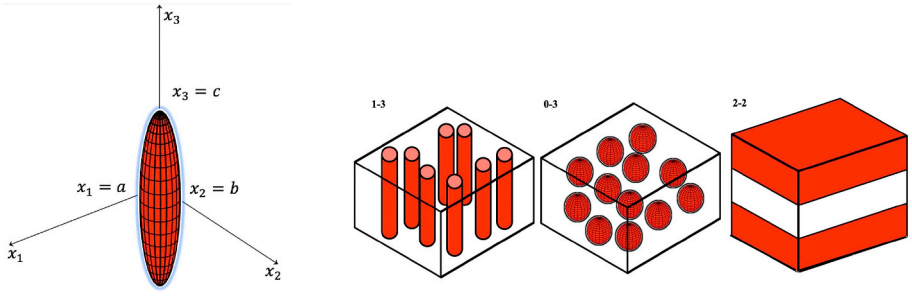

(a) (b)

Fig. 2. Piezocomposite illustration: (a) Ellipsoidal inclusion and (b) illustration of composites with various connectivities.

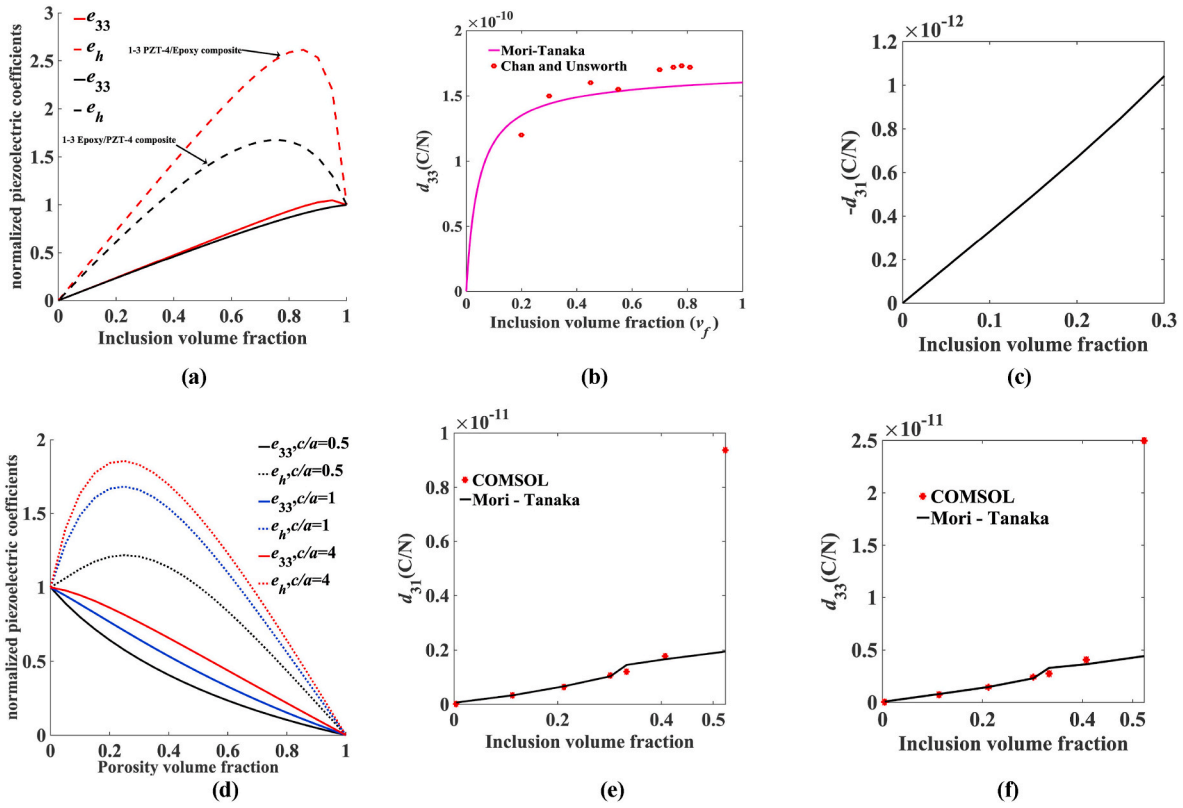

Fig. 3. Checks against previous works: (a) e_h and e_{33} composite calculations for PZT-4/Epoxy composite [2], (b) d_{33} calculations from Mori - Tanaka model for PZT-7A fibers in Epoxy matrix [2] compared with experimental results of Chan et al. [29], (c)−d_{31} calculations for spherical PZT-5 inclusions in Araldite polymer matrix [2], (d) d_{33} calculation for spherical PZT-4 inclusions in Epoxy matrix performed using COMSOL software and (d) d_{31} calculation for spherical PZT-4 in Epoxy matrix performed using COMSOL software.

Table 1
Material moduli of various ceramics and polymer materials used for calculations.

Material	C_{11} (Gpa)	C_{12} (Gpa)	C_{13} (Gpa)	C_{33} (Gpa)	C_{44} (Gpa)	e_{31} (C/m^2)	e_{33} (C/m^2)	e_{15} (C/m^2)	κ_{11}/κ_o-	κ_{33}/κ_o-
PZT-4	139	77.8	74.3	115	25.6	−5.2	15.1	12.7	730	635
PZT-5	121	75.4	75.2	111	21.1	−5.4	15.8	12.3	916	830
PZT-7	148	76.2	74.2	131	25.4	−2.324	9.5	9.2	730	635
Epoxy	6.43	4.29	4.29	6.43	1.07	0	0	0	5	5
Araldite	3.86	2.57	2.57	3.86	0.64	0	0	0	9	9

3.2. Spherical inclusions with scaled properties

We start with a composite comprising spherical piezoelectric inclusions ($c/a = 1$) embedded in a piezoelectric matrix of the same material, subjecting the inclusions to a uniform scaling of all material moduli by a factor α, as defined in equation (27). The volume fraction f of inclusions is varied in the range 0.1–0.5.

Fig. 4 shows homogenized properties of the resulting composites using Mori - Tanaka theory along with results from Hill's homogenization (in dashed lines) for a volume fraction of inclusions $f = 0.1$. Note the similar trend both theories predict at this volume fraction for all performance parameters shown in Fig. 4. Though the trends predicted by the theory of Mori - Tanaka seem to persist in results from Hill's theory, the exact magnitudes differ considerably. It is worth noting that the former has a much better agreement with finite element calculations [15]. Referring to Fig. 4(a) it can be seen that scaling of the inclusion properties can enhance the e_{33} coefficient of the composite, as may be expected. However, the effect is relatively weak: even when the inclusion component has piezoelectric coefficient 100 times greater than those of the matrix material, the homogenized piezoelectric coefficients increase by only a factor of 1.3–3.5, depending on volume fraction. At first sight this appears surprising: placing inclusions with increased piezoelectric response into a composite may not greatly enhance the piezoelectricity of the composite. To understand why this is, it is instructive to consider the distribution of electric field in such a composite. Suppose $\alpha = 100$; then the inclusions are strongly piezoelectric but also have high stiffness and permittivity. The consequence of the high permittivity inclusions on the distribution of electric field is that the electric field strength is low in the inclusions in order to satisfy continuity of electric displacement. Thus, the inclusions contribute little to the development of stress through the piezoelectric effect, while the matrix material dominates the response. This is pertinent to the design of composites in which electroceramic particles are embedded in a polymeric matrix; the electroceramic not only has much greater piezoelectric response than the matrix, but typically also has much greater permittivity. To achieve more fully the advantage in piezoelectric effect that the piezoelectric inclusions can give, the inclusions should experience the full strength of the electric field; this can be achieved in aligned fibre composites. Turning to the piezoelectric coefficient d_{33}, Fig. 4(b) shows that this coefficient of the composite, of importance in displacement actuators and pressure sensors, is largely unchanged by α scaling over a wide range. This is because of the way the d coefficient relates to the stiffness and piezoelectric tensors C and e. Subjecting C and e to any magnitude of uniform scaling results in the expression $\mathbf{d} = \mathbf{C}^{-1}\mathbf{e}$

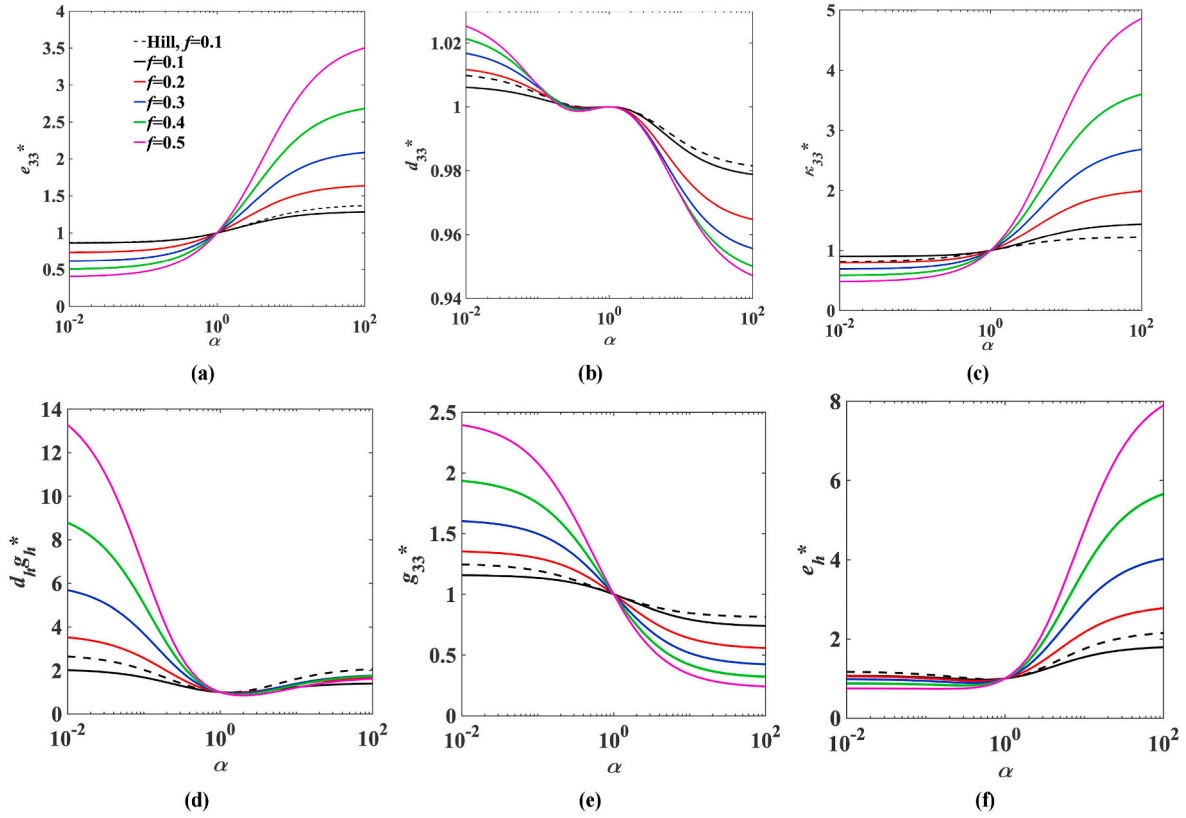

Fig. 4. The effect of α scaling of the electroelastic moduli for spherical piezoelectric inclusions in a piezoelectric matrix. Note that the dashed lines in this figure represent corresponding calculations using Hill's homogenization method.

remaining unchanged. There are slight variations in d_{33} in the composite due to the coupled interactions between matrix and inclusions. Like d_{33}, the electromechanical coupling coefficient k_t shows only slight changes in response to property scaling, remaining in the range of 0.5–0.55 over a wide range of α scaling. The coupling coefficient measures the efficiency with which mechanical energy is converted to electrical energy. When $\alpha < 1$, the inclusion becomes both mechanically compliant and weakly piezoelectric. The inclusion is easily deformed but not sufficiently piezoelectric to convert deformation energy into electrical energy; as a result, it contributes little to the coupling coefficient of the whole composite. Conversely, when $\alpha > 1$, the inclusion becomes strongly piezoelectric but also mechanically stiff. In this case, the increased stiffness limits deformation and hence limits conversion of mechanical to electrical energy even though the inclusion is strongly piezoelectric. Fig. 4(c) show that the dielectric permittivity κ_{33} of the composite can reach a peak value several times that of the base material. Increased permittivity translates to increased charge storage for potential capacitor applications. However, this requires inclusions that have greatly enhanced permittivity. Applications requiring high permittivity do not benefit from formation of a composite as there is always one component of the composite with greater permittivity than the homogenized medium. At the other end of the spectrum of scaling, low κ materials, of importance in microelectronics [30], can be obtained through the incorporation of low κ inclusions into a solid; this could be realized through porous materials [31]. In the design of sonar transducers, the figure of merit $d_h g_h$ ($d_h = d_{33} + d_{31} + d_{32}$, $gh = d_h/\kappa_{33}$) quantifies the efficiency as a transmitter and receiver. Fig. 4(d) indicates that α scaling with $\alpha < 1$ can have a strong effect on this performance parameter. This effect comes primarily from the g coefficients, which increase as α is reduced below unity. The result is of importance to transducer design, indicating that inclusions with minimized moduli are desirable. Consequently, porous piezoelectrics offer enhanced performance as hydrostatic transducers. Next, consider the effect of α scaling on the g_{33} piezoelectric coefficient ($g_{33} = d_{33}/\kappa_{33}$) which is of significance in sensing applications, piezoelectric ignition and energy harvesting from stress. Since this coefficient arises from the inverse of the electroelastic moduli in E, α scaling has a reciprocal effect on g, such that the greatest g coefficients in the inclusion are obtained as $\alpha \to 0$. This effect can be seen in the homogenized composite, as shown in Fig. 4(e). The hydrostatic component e_h exhibits similar behaviour to e_{33}, see Fig. 4(f).

Remaining with spherical inclusions, Fig. 5 shows the effect of a biased scaling, β, of the stiffness tensor C_{ijmn} in the electroelastic modulus E_{iJMn} of the inclusions, keeping piezoelectric and dielectric properties fixed. This enables identification of the restricted influence of inclusion stiffness on the coupled properties of the composite. Starting with the d_{33} coefficient, we see a decreasing trend with increasing $\beta > 1$ at all inclusion volume fractions. This results because stiff inclusions limit local straining, thus constraining coupled effects in the composite. Conversely when $\beta < 1$ the inclusions are mechanically compliant while retaining strong piezoelectricity. This gives rise to increased piezoelectric coupling in the homogenized composite, but note that for typical piezoelectrics, only a modest scaling below $\beta = 1$ is possible before positive definiteness of the inclusion material matrix is lost (dashed lines in Fig. 5), representing materials that are not thermodynamically stable, and thus unlikely to be realized. Similar trends persist in the transducer figure of merit, $d_h g_h$, coupling coefficient, k_t, and the g_{33} coefficient, see Fig. 5(b–d).

When subjected to a biased scaling of the piezoelectric tensor e_{imn}, both d_{33} and $d_h g_h$ show an increase over a range of β with a peak around $\beta = 3$; this is again in an inaccessible range of material properties due to loss of positive definiteness. The coupling coefficient (Fig. 6(c)) shows a similar increase around $\beta = 3$. The initial peak in this range may be the result of an enhanced piezoelectricity which translates to more input mechanical energy being converted to electrical energy.

Turning to a β scaling of the permittivity tensor κ, we see that the

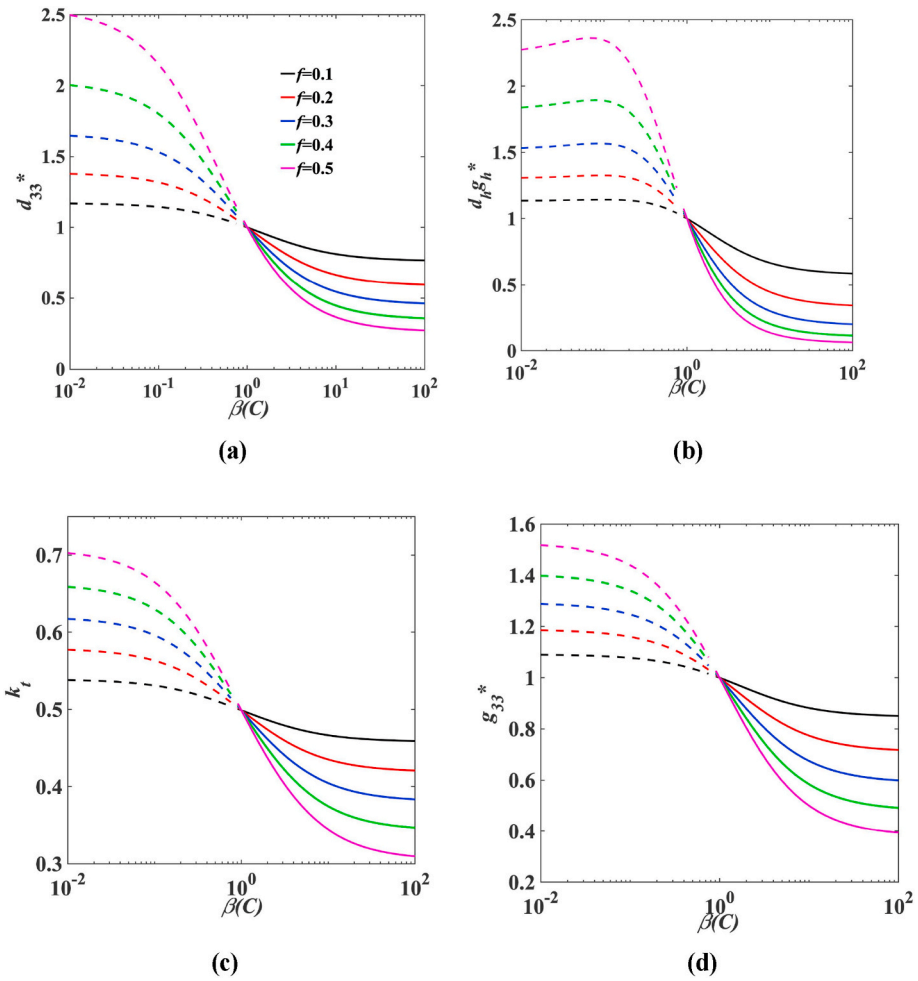

Fig. 5. The effect of β scaling of stiffness tensor C for spherical piezoelectric inclusions in a piezoelectric matrix. Dashed lines indicate loss of positive definiteness of the electroelastic moduli.

transducer figure of merit $d_h g_h$ increases modestly with decreasing dielectric properties in Fig. 7(a) and a similar trend is seen for the g_{33} coefficient, Fig. 7(c). As expected, a biased scaling of the dielectric properties of the inclusion directly affects the κ_{33} permittivity component of the homogenized composite as can be seen in Fig. 7(b). However in a particulate composite the effect on the homogenized medium is much less than the scaling of the inclusions. Thus, for achieving a high permittivity, the formation of the composite is not advantageous. Note that scaling with $\beta << 1$ is largely inaccessible due to loss of positive definiteness. Thus, overall, only limited gains are seen through β scaling of the dielectric properties.

3.3. Rod-shaped and disc-shaped inclusions

We next consider variations of the aspect ratio c/a to produce rod-shaped ($c/a = 10^2$) or disc-shaped ($c/a = 10^{-2}$) inclusions. Fig. 8 summarizes results for both uniform α scaling and biased β scaling of the electroelastic moduli in the inclusions, at various aspect ratios; the inclusion volume fraction is fixed at $f = 0.5$ for the purposes of illustration. Fig. 8(a) reproduces selected results for spherical inclusions ($c/a = 1$) to facilitate comparison with different aspect ratios. The greatest increases in the sonar transducer figure of merit $d_h g_h$ result from a uniform scaling to reduce all properties, implying that the limiting case of spherical pores in a piezoelectric matrix would be beneficial for the design of a sonar transducer. This is consistent with previous modelling results in the literature [31] and some recent experimental investigations [32]. Comparing with Fig. 8(b–c), it is evident that the enhancement of $d_h g_h$ is strongly dependent on the aspect ratio of the inclusions. The greatest benefit to the transducer figure of merit arises when c/a and α are both minimized – corresponding to flat, disc-shaped porosity in the transducer. A comparison with the predictions from laminate theory ($c/a \rightarrow 0$) is shown in Fig. 8(b), indicating a similar trend with scaling. The results suggest that thin, crack-like pores in the piezoelectric matrix could be beneficial for increasing the transducer figure of merit; this contrasts with some conventional designs that employ rod-shaped piezoelectric inclusions in a polymer matrix [33]. A similar degree of improvement was recently reported in a more complex composite of piezoelectric inclusions in a porous polymer matrix with two different types of pores by Topolov et al. [34]. The findings may indicate a route for development of improved transducer materials, though it should be noted that the theory proceeds on the assumptions of continuity of electric displacement and linear material behaviour. In the limit of thin, flat porosity, the electric field strength in the pores may result in charge transfer across pores (electrical breakdown) which could limit the applicability of this material design. Thus the porosity may require highly insulating properties to achieve the effect indicated in Fig. 8(b), suggesting the use of polymer inclusions with high breakdown strength. A rod-shaped geometry for the inclusions, Fig. 8(c), shows similar trends but with less enhancement to the figure of merit. Fig. 8 suggests that a uniform α scaling of the electroelastic moduli would have a greater influence on the transducer performance than any individual biased β property scaling.

The longitudinal piezoelectric coefficient d_{33} follows a different pattern to that of the figure of merit $d_h g_h$. Comparing the α scaling alone

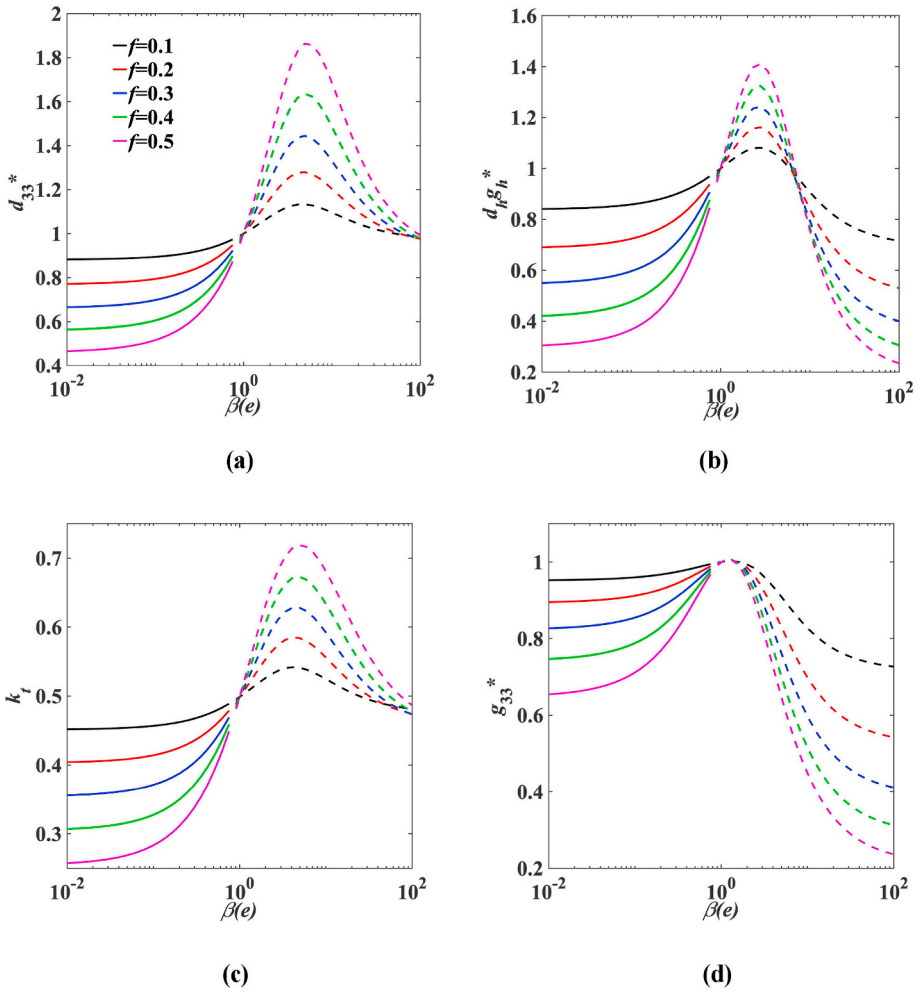

Fig. 6. The effect of β scaling of piezoelectric tensor e for spherical piezoelectric inclusions in a piezoelectric matrix. Dashed lines indicate loss of positive definiteness of the electroelastic moduli.

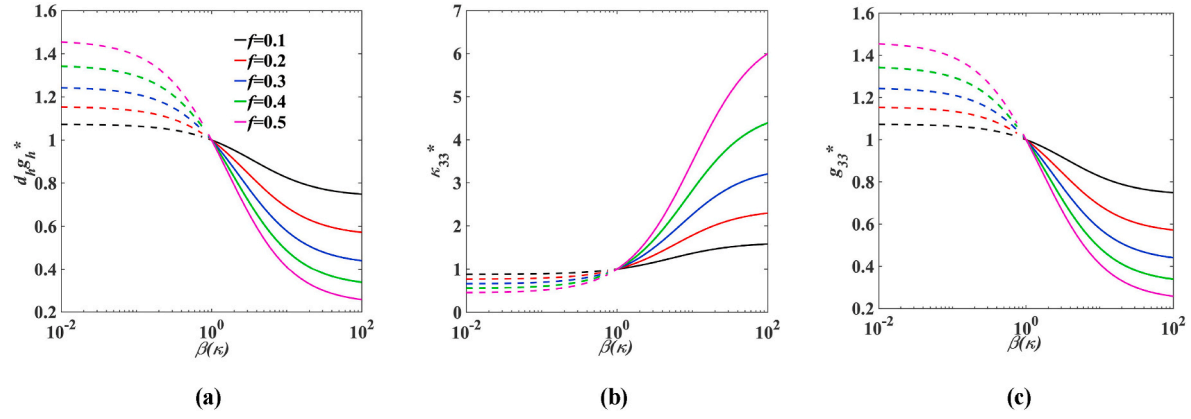

Fig. 7. The effect of β scaling of dielectric tensor κ for spherical piezoelectric inclusions in a piezoelectric matrix. Dashed lines indicate loss of positive definiteness of the electroelastic moduli.

throughout the three aspect ratios shown in Fig. 9, it can be seen that the d_{33} coefficient of the composite is almost unchanged by scaling of the electroelastic moduli of the inclusion. Consistent results in the case $c/a = 0.01$ are obtained using laminate theory in Fig. 9(b). If instead, a biased scaling of stiffness with $\beta < 1$ is applied, this improves the d_{33} performance for all aspect ratios, with the greatest increase occurring in the case of disc-shaped inclusions ($c/a = 0.01$). An even greater enhancement of d_{33} appears in rod-shaped inclusions with $\beta > 1$ scaling of the piezoelectric coefficients. However, note that these enhancements may not be realizable due to thermodynamic limits. Biased scaling of the dielectric properties appears to have negligible influence on the d_{33} coefficient of the composite.

Fig. 10 shows the effect of various types of scaling and inclusion aspect ratios on the electromechanical coupling coefficient k_t. The

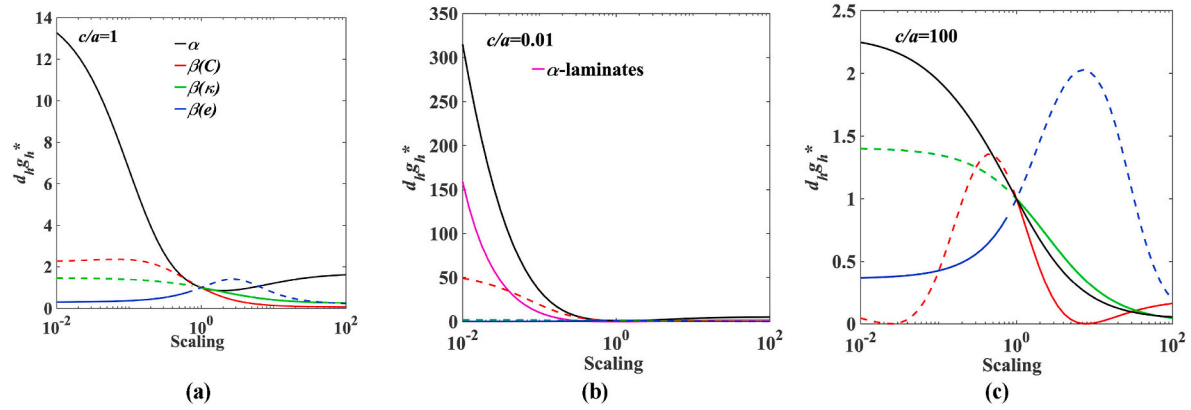

Fig. 8. The effect of α and β scaling on figure of merit $d_h g_h$ for varying aspect ratios, c/a, of inclusions. The inclusion volume fraction is fixed at 0.5. Dashed lines indicate loss of positive definiteness of the electroelastic moduli.

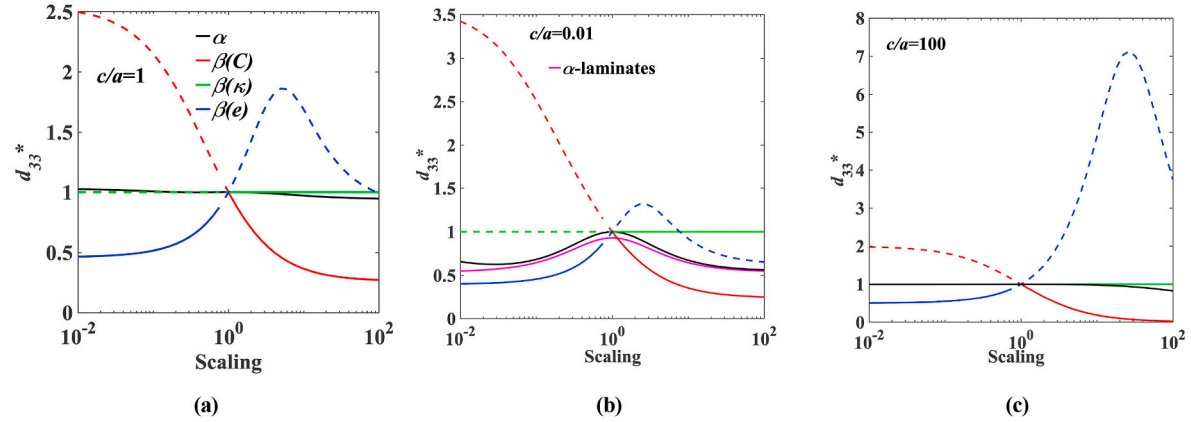

Fig. 9. The effect of α and β scaling on the longitudinal piezoelectric coefficient d_{33} for varying aspect ratios, c/a, of inclusions. The inclusion volume fraction is fixed at 0.5. Dashed lines indicate loss of positive definiteness of the electroelastic moduli.

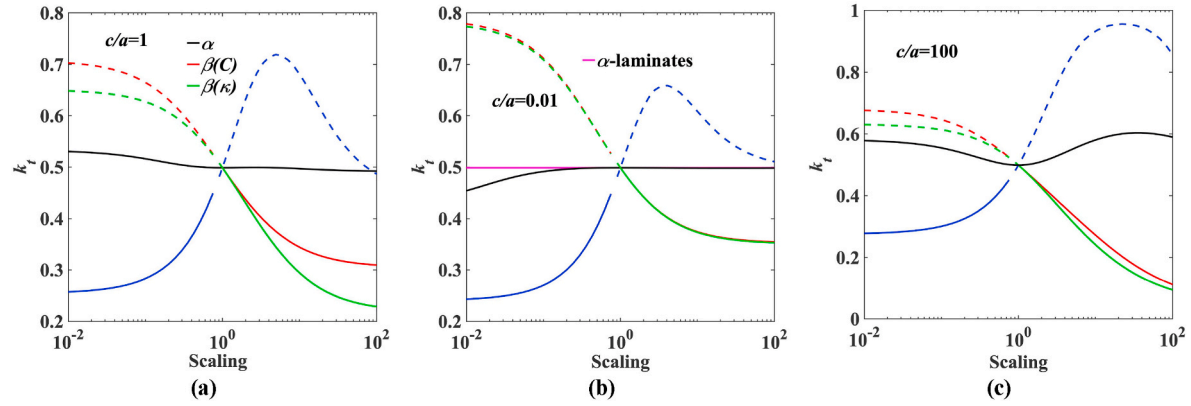

Fig. 10. The effect of α and β scaling on coupling coefficient k_t for varying aspect ratios, c/a, of inclusions. The inclusion volume fraction is fixed at 0.5. Dashed lines indicate loss of positive definiteness of the electroelastic moduli.

coupling coefficient is largely unchanged by α scaling for all aspect ratios. It increases significantly with either biased scaling of stiffness or permittivity when $\beta < 1$, or biased scaling of the piezoelectric coefficients when $\beta > 1$. Significant gains appear for all inclusion aspect ratios, but note that the practically achievable gains are again strongly limited by loss of positive definiteness.

The effect of material property scaling and inclusion aspect ratio on the dielectric permittivity κ_{33} is shown in Fig. 11.

Uniform scaling with $\alpha > 1$ increases the permittivity. This implies that stiffening the inclusion while strengthening both its piezoelectric and dielectric properties is favourable if a higher overall permittivity for the composite is desired. A scaling in stiffness alone, β (C), leaves the permittivity of the composite largely unchanged for all aspect ratios of inclusions. However, biased increase of the piezoelectric properties, β $(e) > 1$, increases the composite permittivity with striking results in the case of rod-shaped inclusions. Once again, thermodynamic stability limits the available gains.

In Fig. 12, we see that disc-shaped porosity has potential benefits to

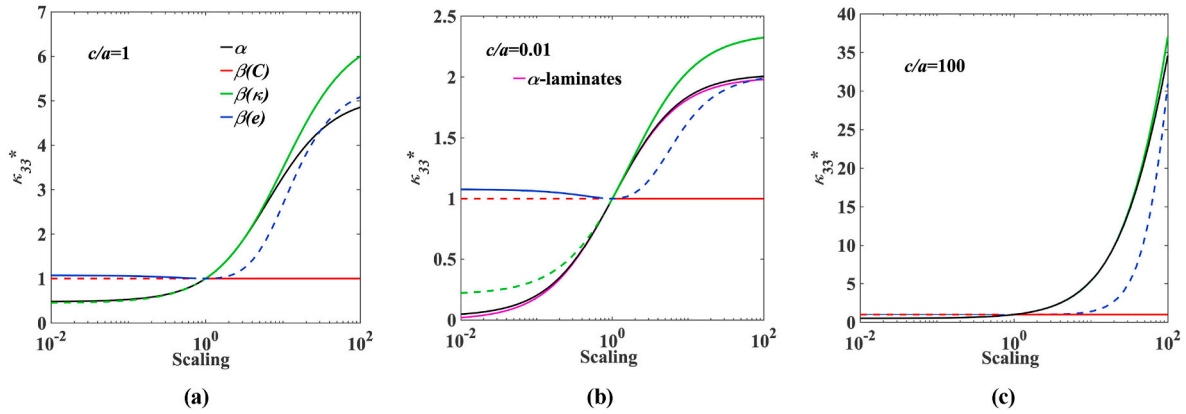

Fig. 11. The effect of α and β scaling on dielectric tensor κ_{33} for varying aspect ratios, c/a, of inclusions. The inclusion volume fraction is fixed at 0.5. Dashed lines indicate loss of positive definiteness of the electroelastic moduli.

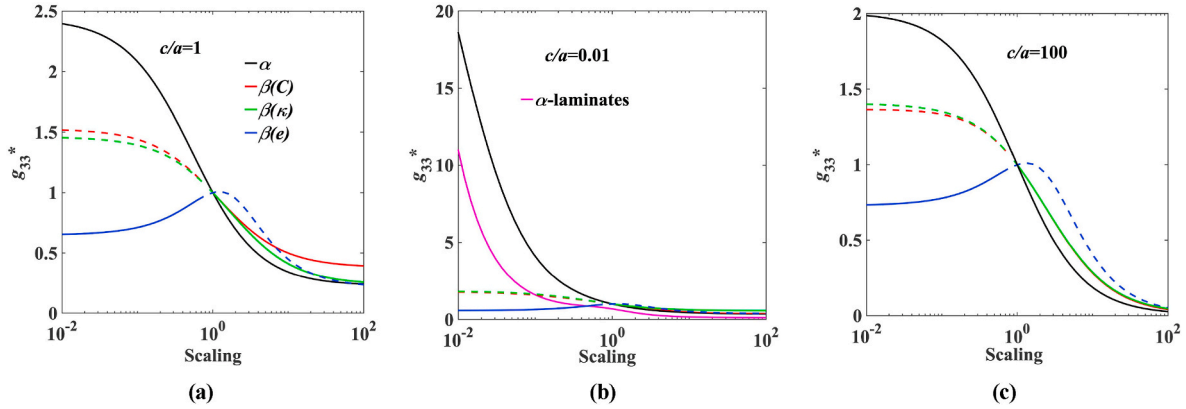

Fig. 12. The effect of α and β scaling on piezoelectric coefficient g_{33} for varying aspect ratios, c/a, of inclusions. The inclusion volume fraction is fixed at 0.5. Dashed lines indicate loss of positive definiteness of the electroelastic moduli.

the g_{33} performance of a composite at $\alpha < 1$ and $c/a = 0.01$. Biased scaling of stiffness or dielectric permittivity produce similar effects on the g_{33} piezoelectric coefficient. Interestingly, a biased scaling of the piezoelectricity tensor e has relatively little influence on the overall g_{33} piezoelectric coefficient.

To conclude the study, we provide a comparison of the model with recent experimental data of Zhang et al. [13]. Porous transducers are of great interest as they can offer a superior figure of merit $d_h g_h$ to that of a bulk ceramic. It was demonstrated in the aforementioned work that a porous BCZT (barium titanate doped with Ca, Zr) based composition offered a performance over 100 times that of the dense ceramic. A comparison between predictions of the Mori - Tanaka model and these experimental results is presented in Fig. 13.

In order to model the experimental data, ideally the full electroelastic moduli of the matrix material would be used. As these were not available, estimates were based on the known elastic, piezoelectric and dielectric properties of barium titanate, which were modified by scaling the e_{ijk} and κ_{ik} tensors by a factor of $\beta(e) = \beta(\kappa) = 3$ to reflect the reported experimental value of $d_{33} = 600$ pC/N[13,32]. Regarding the stiffness C_{ijkl} of BCZT, it is likely that it is not as high as 3 times that of barium titanate, as evidenced in literature relating to doped barium titanates [35]. The stiffness of BCZT is expected to lie in the range of 1–1.5 times that of barium titanate [32]. Note that introducing porosity also modifies the stiffness, especially at higher porosity levels, at which point the Mori - Tanaka model might not adequately capture the consequent matrix compliance [16]. Accordingly, we vary the stiffness in the range 0.5–1.7 in order provide a reasonable fit to the experimental data. As for the aspect ratio c/a, we found a better fit for the experimental data with oblate ($c/a < 1$) rather than prolate ($c/a > 1$) inclusions. The experimental data [13] indicates the presence of a variety of irregular pore shapes in this BCZT ceramic; we show calculations for $c/a = 0.1$, 0.3 and 0.5. As can be seen in Fig. 13, the agreement in the trends across all piezoelectric coefficients is reasonable given many uncertainties about the details of the porous BCZT. The general agreement with complex experimental data gives some confidence in the model's ability to capture trends in the behaviour of real composites.

4. Conclusions

A simple two-component piezocomposite comprising piezoelectric matrix and inclusion materials was studied, with the inclusion material subjected to a uniform scaling (α) or biased scaling (β) of the electroelastic moduli. The objective was to study the effects of property-contrast between constituent components on piezoelectric performance. The results of scaling on various piezoelectric coefficients and performance parameters were explored across a range of inclusion geometries. It was found that penny shaped pores in a piezoelectric ceramic can produce remarkable enhancement of $d_h g_h$, by factors of several hundred relative to the dense ceramic. Scaling of the electroelastic moduli uniformly or in a biased manner does not always have straightforward consequences for the behaviour of the composite. Uniform scaling of all electroelastic moduli of the inclusions benefited certain performance coefficients, but the piezoelectric coefficient d_{33} is almost unaffected by this scaling. Meanwhile, a biased contrast in any one of the elastic, piezoelectric and dielectric properties between the components proved detrimental to most performance parameters.

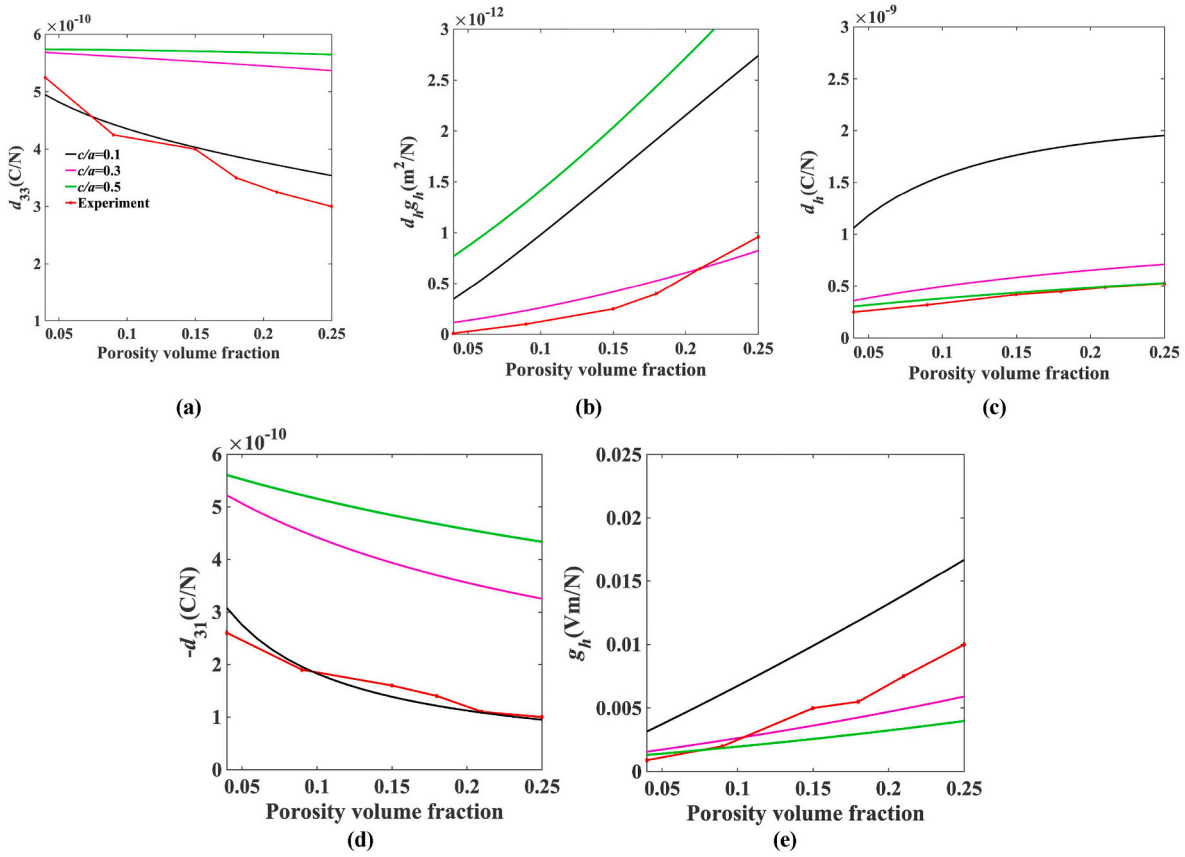

Fig. 13. Trends shown in Mori - Tanaka calculations and experimental measurements of porous BCZT ceramic by Zhang et al. [13].

Noting that porous ceramics (represented approximately by uniform scaling $\alpha = 10^{-2}$) can produce excellent performance for the transducer figure of merit $d_h g_h$, the present model was used for comparison with recent experimental results for porous BCZT ceramics, with a satisfactory fit to the experimental data. This illustrates the utility of property contrast as a concept for modelling the performance of piezoelectric composites. The results of this study contribute insight into piezoelectric composites that can provide guidance for future design of transducer materials. By highlighting remarkable performance improvements resulting from modifying a few material parameters, the study also points to an opportunity for more generalized optimization of piezoelectric composites. In summary, the findings of the present work are: (1) Uniform contrast between matrix and inclusion in a two-component composite show functional performance enhancements that are accessible, (2) The transducer figure of merit $d_h g_h$ in particular shows a giant enhancement resulting of minimized material moduli of the inclusions, (3) Biased contrast between matrix and inclusion does boost some functional performance parameters but these are inaccessible as they breach thermodynamic limits and (4) The concept of property contrast was demonstrated to reasonably capture functional performance of a real world ceramic (BCZT).

CRediT authorship contribution statement

Nihal Thafeem Ahmed Faheem Ahmed: Software, Formal analysis, Investigation, Conceptualization, Writing – original draft. **John E. Huber:** Conceptualization, Supervision, Writing – review & editing, Project administration.

Declaration of competing interest

The authors declare that they have no conflict of interest.

Data availability

Material data used will be provided on request.

References

[1] R.Y. Ting, A review on the development of piezoelectric composites for underwater acoustic transducer applications, IEEE Trans. Instrum. Meas. 41 (1992) 64–67.
[2] M.L. Dunn, M. Taya, An analysis of piezoelectric composite materials containing ellipsoidal inhomogeneities, Proc. Royal Soc. London. Ser. A: Math. Phys. Sci. 443 (1993) 265–287.
[3] K. Han, Y. Roh, The performance of a 1–3 mode piezocomposite ultrasonic transducer in relation to the properties of its polymer matrix, Sensors Actuators A: Phys. 75 (1999) 176–185.
[4] Z. Wang, J. Zhu, X. Jin, W. Chen, C. Zhang, Effective moduli of ellipsoidal particle reinforced piezoelectric composites with imperfect interfaces, J. Mech. Phys. Solid. 65 (2014) 138–156.
[5] A. Pan'kov, Piezocomposite with reciprocal polarization of oriented ellipsoidal inclusions and the matrix, Mech. solids 45 (2010) 247–256.
[6] V.Y. Topolov, A. Turik, Porous piezoelectric composites with extremely high reception parameters, Tech. Phys. 46 (2001) 1093–1100.
[7] J. Xu, L. Wang, C. Zhong, The effect of piezoceramic volume fraction on properties of three-phase piezocomposites, Ferroelectrics 555 (2020) 132–145.
[8] J.H. Huang, W.-S. Kuo, Micromechanics determination of the effective properties of piezoelectric composites containing spatially oriented short fibers, Acta Mater. 44 (1996) 4889–4898.
[9] C.Y. Kiyono, E.C.N. Silva, J. Reddy, Design of laminated piezocomposite shell transducers with arbitrary fiber orientation using topology optimization approach, Int. J. Numer. Methods Eng. 90 (2012) 1452–1484.
[10] T. Mori, K. Tanaka, Average stress in matrix and average elastic energy of materials with misfitting inclusions, Acta Metall. 21 (1973) 571–574.
[11] Y. Benveniste, The determination of the elastic and electric fields in a piezoelectric inhomogeneity, J. Appl. Phys. 72 (1992) 1086–1095.
[12] C.N. Della, D. Shu, The performance of 1–3 piezoelectric composites with a porous non-piezoelectric matrix, Acta Mater. 56 (2008) 754–761.
[13] Y. Zhang, M. Xie, J. Roscow, C. Bowen, Dielectric and piezoelectric properties of porous lead-free $0.5Ba(Ca_{0.8}Zr_{0.2})O_3$- $0.5(Ba_{0.7}Ca_{0.3})TiO_3$, Mater. Res. Bull. 112 (2019) 426–431.

[14] F. Dinzart, H. Sabar, Electroelastic ellipsoidal inclusion with imperfect interface and its application to piezoelectric composite materials, Int. J. Solid Struct. 136 (2018) 241–249.
[15] G.M. Odegard, Constitutive modeling of piezoelectric polymer composites, Acta Mater. 52 (2004) 5315–5330.
[16] M.L. Dunn, M. Taya, Electromechanical properties of porous piezoelectric ceramics, J. Am. Ceram. Soc. 76 (1993) 1697–1706.
[17] A. Jafari, A.A. Khatibi, M.M. Mashhadi, Comprehensive investigation on hierarchical multiscale homogenization using representative volume element for piezoelectric nanocomposites, Composites, Part B 42 (2011) 553–561.
[18] V.Y. Topolov, A. Turik, Nonmonotonic concentration dependence of piezoelectric coefficients of 1–3 composites, J. applied physics 85 (1999) 372–379.
[19] J. Yang, et al., An Introduction to the Theory of Piezoelectricity, vol. 9, Springer, 2005.
[20] J.R. Barber, Elasticity, Springer, 2002.
[21] D. Barnett, J. Lothe, Dislocations and line charges in anisotropic piezoelectric insulators, Phys. Status Solidi 67 (1975) 105–111.
[22] R. Hill, A self-consistent mechanics of composite materials, J. Mech. Phys. Solid. 13 (1965) 213–222.
[23] J.D. Eshelby, The determination of the elastic field of an ellipsoidal inclusion, and related problems, Proc. royal society London. Ser. A. Math. physical sciences 241 (1957) 376–396.
[24] W.F.J. Deeg, The Analysis of Dislocation, Crack, and Inclusion Problems in Piezoelectric Solids, Stanford University, 1980.
[25] J.H. Huang, J. Yu, Electroelastic eshelby tensors for an ellipsoidal piezoelectric inclusion, Compos. Eng. 4 (1994) 1169–1182.
[26] J. Huber, N. Fleck, C. Landis, R. McMeeking, A constitutive model for ferroelectric polycrystals, J. Mech. Phys. Solid. 47 (1999) 1663–1697.
[27] J. Li, D. Liu, On ferroelectric crystals with engineered domain configurations, J. Mech. Phys. Solid. 52 (2004) 1719–1742.
[28] V.Y. Topolov, C.R. Bowen, Electromechanical Properties in Composites Based on Ferroelectrics, Springer Science & Business Media, 2008.
[29] H.L.W. Chan, J. Unsworth, Simple model for piezoelectric ceramic/polymer 1-3 composites used in ultrasonic transducer applications, IEEE Trans. Ultrason. Ferroelectrics Freq. Control 36 (1989) 434–441.
[30] K. Maex, et al., Low dielectric constant materials for microelectronics, J. Appl. Phys. 93 (2003) 8793–8841.
[31] M.R. Baklanov, K. Maex, Porous low dielectric constant materials for microelectronics, Phil. Trans. Math. Phys. Eng. Sci. 364 (2006) 201–215.
[32] Z. Rymansaib, et al., Ultrasonic transducers made from freeze-cast porous piezoceramics, IEEE Trans. Ultrason. Ferroelectrics Freq. Control 69 (2022) 1100–1111.
[33] R. Pramanik, A. Arockiarajan, Effective properties and nonlinearities in 1-3 piezocomposites: a comprehensive review, Smart Mater. Struct. 28 (2019) 103001.
[34] V.Y. Topolov, A.N. Isaeva, P. Bisegna, Squared figures of merit and electromechanical coupling factors of a novel lead-free 1–3–0 composite for sensor and energy-harvesting applications, Sensors Actuators A: Phys. 318 (2021) 112473.
[35] A.J. Moulson, J.M. Herbert, Electroceramics: Materials, Properties, Applications, John Wiley & Sons, 2003.